Cell Reports
Article

Cell PRESS
Open ACCESS

Hypoxia Induces VEGF-C Expression in Metastatic Tumor Cells via a HIF-1α-Independent Translation-Mediated Mechanism

Florent Morfoisse,[1,2] Anna Kuchnio,[3] Clement Frainay,[1,2] Anne Gomez-Brouchet,[1,2] Marie-Bernadette Delisle,[1,2] Stefano Marzi,[4] Anne-Catherine Helfer,[4] Fransky Hantelys,[5] Francoise Pujol,[5] Julie Guillermet-Guibert,[1,2] Corinne Bousquet,[1,2] Mieke Dewerchin,[3] Stephane Pyronnet,[1,2] Anne-Catherine Prats,[5,6] Peter Carmeliet,[3,6] and Barbara Garmy-Susini[1,2,*]

[1]Inserm, U1037, 31432 Toulouse, France
[2]Université de Toulouse, UPS, Cancer Research Center of Toulouse, Equipe Labellisee Ligue Contre le Cancer and Laboratoire d'Excellence Toulouse Cancer, 31432 Toulouse, France
[3]Vesalius Research Center, VIB, University of Leuven, 3000 Leuven, Belgium
[4]UPR 9002 CNRS-ARN, Université De Strasbourg, IBMC, 67084 Strasbourg, France
[5]Université de Toulouse, UPS, TRADGENE, EA4554, 31432 Toulouse, France
[6]These authors contributed equally to this work
*Correspondence: barbara.garmy-susini@inserm.fr
http://dx.doi.org/10.1016/j.celrep.2013.12.011

SUMMARY

Various tumors metastasize via lymph vessels and lymph nodes to distant organs. Even though tumors are hypoxic, the mechanisms of how hypoxia regulates lymphangiogenesis remain poorly characterized. Here, we show that hypoxia reduced vascular endothelial growth factor C (VEGF-C) transcription and cap-dependent translation via the upregulation of hypophosphorylated 4E-binding protein 1 (4E-BP1). However, initiation of VEGF-C translation was induced by hypoxia through an internal ribosome entry site (IRES)-dependent mechanism. IRES-dependent VEGF-C translation was independent of hypoxia-inducible factor 1α (HIF-1α) signaling. Notably, the VEGF-C IRES activity was higher in metastasizing tumor cells in lymph nodes than in primary tumors, most likely because lymph vessels in these lymph nodes were severely hypoxic. Overall, this transcription-independent but translation-dependent upregulation of VEGF-C in hypoxia stimulates lymphangiogenesis in tumors and lymph nodes and may contribute to lymphatic metastasis.

INTRODUCTION

The lymphatic vasculature consists of a network of lymph vessels that drain interstitial fluid from tissues and return it to the blood. It is also essential for immune surveillance. However, increased lymphangiogenesis also contributes to tumor metastasis and various inflammatory diseases, while insufficient lymph vessel growth or dysfunction causes lymphedema (Albrecht and Christofori, 2011; Alitalo, 2011; Bonnal et al., 2003; Christiansen and Detmar, 2011; Martinez-Corral and Makinen, 2013). Blocking lymphangiogenesis may offer therapeutic benefit to limit tumor spread.

Hypoxia promotes the growth of blood vessels (angiogenesis), but only limited data are available on whether and how hypoxia regulates lymphangiogenesis. Nevertheless, lymph vessels are often located in remote areas away from oxygen-carrying blood vessels and do not contain oxygen-carrying red blood cells; they are thus exposed to a milieu with very low oxygen levels (Guzy et al., 2008; Ivanovic, 2009). Some correlative studies suggest a link among tumor hypoxia, the hypoxia-inducible transcription factor HIF-1α, and lymphangiogenesis (Schoppmann et al., 2006; Tao et al., 2006). Another study reported that HIF-1α promotes lymphatic metastasis by transcriptional activation of the lymphangiogenic factor platelet derived growth factor B (Schito et al., 2012). HIF-1α also stimulates transcription of Prox-1, another lymph-angiogenic factor (Zhou et al., 2013). However, whether hypoxia signaling (and in particular HIF-1α) regulates the expression of vascular endothelial growth factor C (VEGF-C), one of the key lymphangiogenic factors (Alitalo and Detmar, 2012), remains unknown. Only a single report documented an associative correlation between HIF-1α and VEGF-C in cancer (Liang et al., 2008). It is also unknown whether VEGF-C expression in hypoxic conditions relies on transcriptional or translational mechanisms.

When cells are exposed to low oxygen levels, they suppress general protein synthesis in order to save energy (Kaelin and Ratcliffe, 2008; Majmundar et al., 2010; Maxwell, 2005; Semenza, 2012). Hypoxia inhibits mRNA translation by affecting the activity of two kinases, mTOR and PERK (Larsson et al., 2013; Silvera and Schneider, 2009). Inactivation

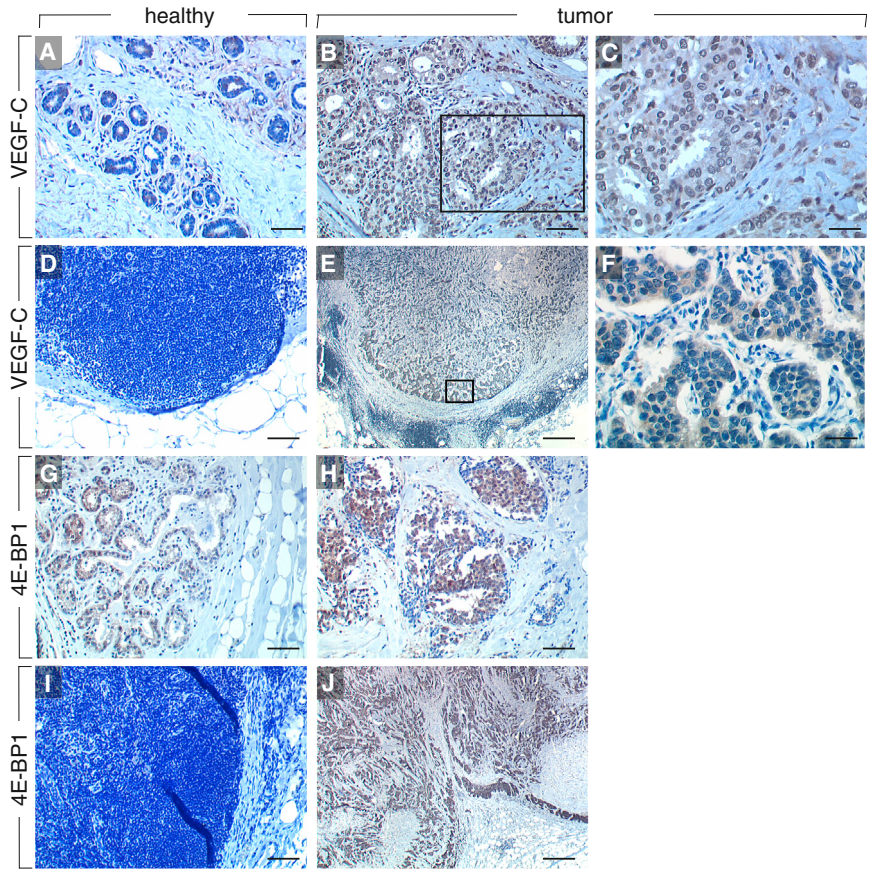

Figure 1. Expression Levels of VEGF-C and 4E-BP1 in Breast Tumor Specimens

(A–F) Immunostaining of VEGF-C in human specimens of healthy breast tissue (A), invasive breast cancer (B and C), and in healthy (D) and metastasized (E and F) lymph nodes. (C) and (F) show larger magnification of the framed area of (B) and (E), respectively.

(G–J) Immunostaining of 4E-BP1 in human healthy breast epithelium (G), invasive breast cancer (H), and normal (I) and metastasized (J) lymph nodes. Scale bar represents 50 μm (A, B, G, and H), 25 μm (C and F), and 250 μm (D, E, I, and J).

of mTOR results in hypophosphorylation of eIF4E-binding proteins (4E-BP), which promotes the sequestering of eIF4E, a factor necessary for cap-dependent translation (Martineau et al., 2013; Richter and Sonenberg, 2005). Hypoxic activation of PERK is mediated by the unfolded protein response and inhibits translation by phosphorylating the translation initiation factor eIF2-α (Koumenis and Wouters, 2006).

Other mRNAs are translated in hypoxic conditions by an alternative mechanism, mediated by internal ribosome entry sites (IRESs) located in their 5′ UTRs, which allows the ribosome to be recruited to a site that is at a considerable distance from the cap structure, most frequently in the presence of *trans*-acting factors (Spriggs et al., 2008; Vagner et al., 2001). Many cellular mRNAs have now been documented to contain IRESs. The majority of identified IRESs are found in mRNAs of proteins that are associated with the control of cell growth and death, including growth factors, proto-oncogenes and proteins required for apoptosis (Bushell et al., 2004). IRES elements have also been identified in VEGF-A and fibroblast growth factor 2 mRNA sequences and are activated by hypoxia to stimulate angiogenesis (Bornes et al., 2007). However, since it is unknown if IRES-dependent expression of VEGF-C in hypoxic conditions regulates lymphangiogenesis, we characterized IRES-dependent induction of VEGF-C in hypoxic tumors and lymph nodes.

RESULTS

Coexpression of VEGF-C and 4E-BP1 in Tumor Cells

We examined by immunohistochemistry (IHC) the expression levels of VEGF-C in human healthy breast specimens, tumor biopsies of invasive ductal carcinomas, and draining metastatic lymph nodes. Fifteen tumor biopsy specimens and their sentinel nodes were analyzed. Immunoreactive VEGF-C levels were moderate in healthy tissues but elevated in tumor samples (Figures 1A–1C). VEGF-C was undetectable in healthy lymph nodes but upregulated in metastatic tumor cells in lymph nodes (Figures 1D–1F).

Notably, 4E-BP1, a negative regulator of cap-dependent mRNA translation, was overexpressed in tumors and metastatic lymph nodes as compared to healthy epithelium and noninvaded lymph nodes (Figures 1G–1J). Since overexpression of 4E-BP1 inhibits cap-dependent translation induced by hypoxia in tumors (Braunstein et al., 2007), these findings raised the question whether VEGF-C translation in tumors and metastatic lymph nodes relied on a cap-independent regulation of VEGF-C translation.

VEGF-C mRNA Is Reduced while VEGF-C Protein Is Increased in Tumors

We used three different mouse tumor models known to induce lymphangiogenesis and to metastasize via lymph vessels: Capan-1, a xenograft of human pancreatic adenocarcinoma; 4T1, an orthotopic syngeneic mouse model of metastatic breast cancer; and a syngeneic subcutaneous model of Lewis lung carcinoma (LLC) (Deer et al., 2010; Garmy-Susini et al., 2010; Pulaski and Ostrand-Rosenberg, 2001). When studying the expression of VEGF-C in primary tumor extracts during tumor progression, we found that VEGF-C mRNA levels were decreased (Figures 2A–2C), while human VEGF-C protein levels were increased in the three tumor cell types, as observed by a human VEGF-C-specific ELISA (Figure 2D) and by immunoblotting (Figures 2E and 2F). These data suggested that induction of VEGF-C expression occurred via a posttranscriptional

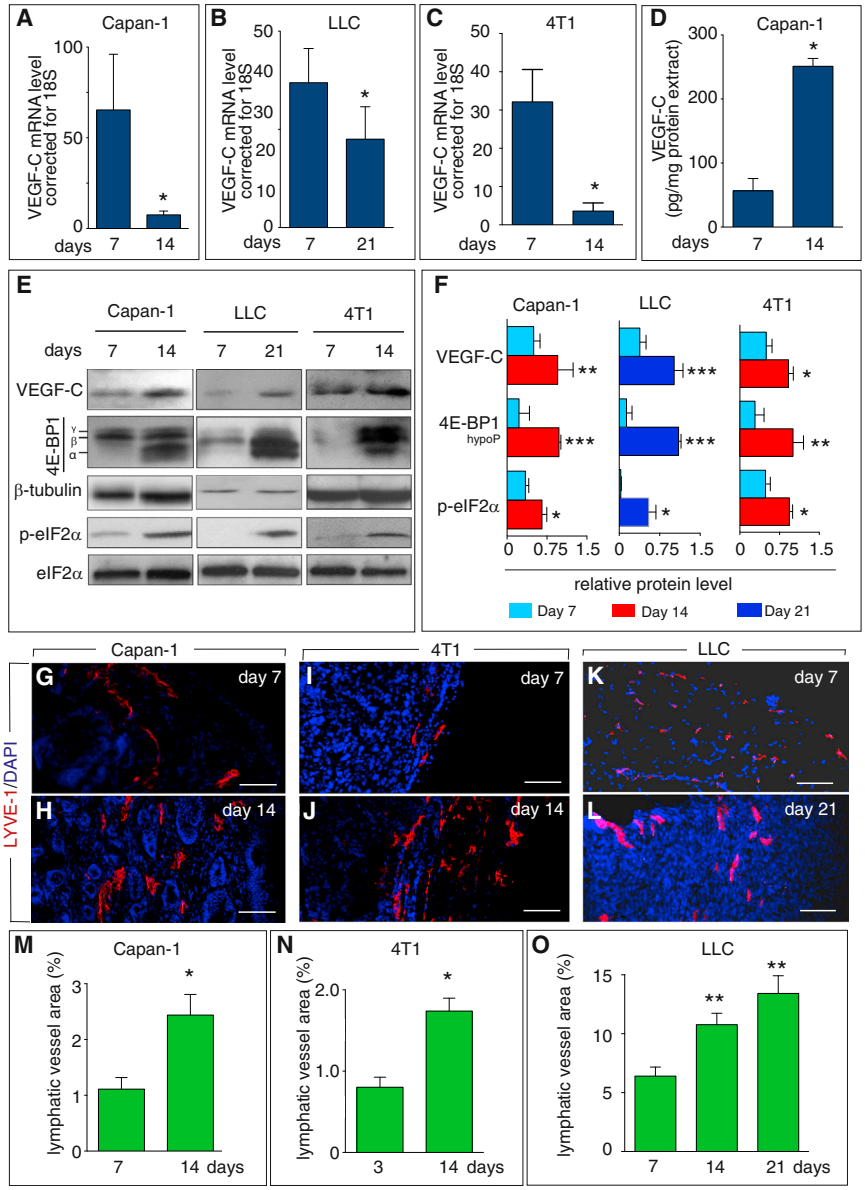

Figure 2. Tumor Lymphangiogenesis Correlates with Posttranscriptional Induction of VEGF-C In Vivo

(A–C) Quantitative RT-PCR (qRT-PCR) of VEGF-C mRNA in Capan-1 pancreatic (A), LLC (B), and 4T1 breast (C) tumors shows a decrease of VEGF-C transcript levels during tumor growth (mean ± SEM; n = 8–10; *p < 0.001).

(D), ELISA analysis showing increased VEGF-C protein levels during Capan-1 tumor growth (mean ± SEM; n = 5, *p < 0.001).

(E and F) Immunoblot of VEGF-C, 4E-BP1, and eIF2α and phosphorylated eIF2α (p-eIF2α) in Capan-1 pancreatic, LLC, and 4T1 breast tumors, showing an increase in VEGF-C protein levels, associated with increased expression and dephosphorylation of 4E-BP1 and with increased phosphorylation of eIF2α when comparing day 14 (Capan-1, 4T1) or day 21 (LLC) with day 7 tumor protein extracts. Quantification by densitometry is shown in (F). Relative levels are normalized to β-tubulin (VEGF-C, hypophosphorylated 4E-BP1) or to eiF2α (p-eiF2α) (mean ± SEM; n = 8–10; *p < 0.05 **p < 0.01, ***p < 0.001).

(G–L) Immunostaining for LYVE-1 (red) demonstrating increased lymphangiogenesis during Capan-1 pancreatic (G and H), 4T1 breast (I and J), and LLC (K and L) growth. Nuclei are visualized by DAPI staining (blue).

(M–O) Morphometric quantification of tumor lymphatic vessel area (% of tumor area) in Capan-1 (M), 4T1 (N), and LLC (O) tumors (mean ± SEM; n = 8–10; *p < 0.01).

Scale bar represents 50 μm (G–L). See also Figure S1.

mechanism. Use of murine VEGF-C-specific primers in the human Capan-1 tumor model revealed that stromal cells did not compensate for the reduced human VEGF-C mRNA levels by upregulating murine VEGF-C transcript levels (Figure S1). Staining for the lymphatic endothelial cell marker LYVE-1 complemented with quantification of lymph vessel area showed that lymphangiogenesis increased during tumor progression (Figures 2G–2O), in agreement with the enhanced VEGF-C protein levels.

We studied the phosphorylation status of 4E-BP1 by immunoblotting. 4E-BP1 can be hypophosphorylated (designated α-form) or hyperphosphorylated (designated β and γ forms). In its hypophosphorylated state, 4E-BP1 inhibits cap-dependent translation initiation by sequestering eIF-4E (Martineau et al., 2013; Richter and Sonenberg, 2005). During tumor progression, total 4E-BP1 protein levels increased and 4E-BP1 became increasingly hypophosphorylated, as evidenced by the shift to a lower molecular weight (Figures 2E and 2F). We also analyzed eIF2α phosphorylation using antibodies recognizing phosphorylated and total eIF2α, as eIF2α phosphorylation downregulates protein synthesis in various stress conditions, including hypoxia (Koumenis and Wouters, 2006). Notably, phosphorylated eIF2α (p-eIF2α) levels increased during tumor progression (Figures 2E and 2F). Thus, decreased VEGF-C mRNA and increased VEGF-C protein levels, together with the decrease of global translation initiation in tumors mediated by 4E-BP and eIF2α, suggested a stress-specific mechanism of regulation of VEGF-C translation, such as an IRES-dependent translation process.

Structure Probing of the 5′ UTR mRNA of VEGF-C

We therefore explored if VEGF-C might be translated via IRES-dependent regulation. In order to analyze if the 5′ UTRs of the human and murine VEGF-C contained conserved structural features, the secondary structures of both RNAs were studied by using "selective 2′-hydroxyl acylation analyzed by primer extension" (SHAPE) analysis to obtain information on the RNA

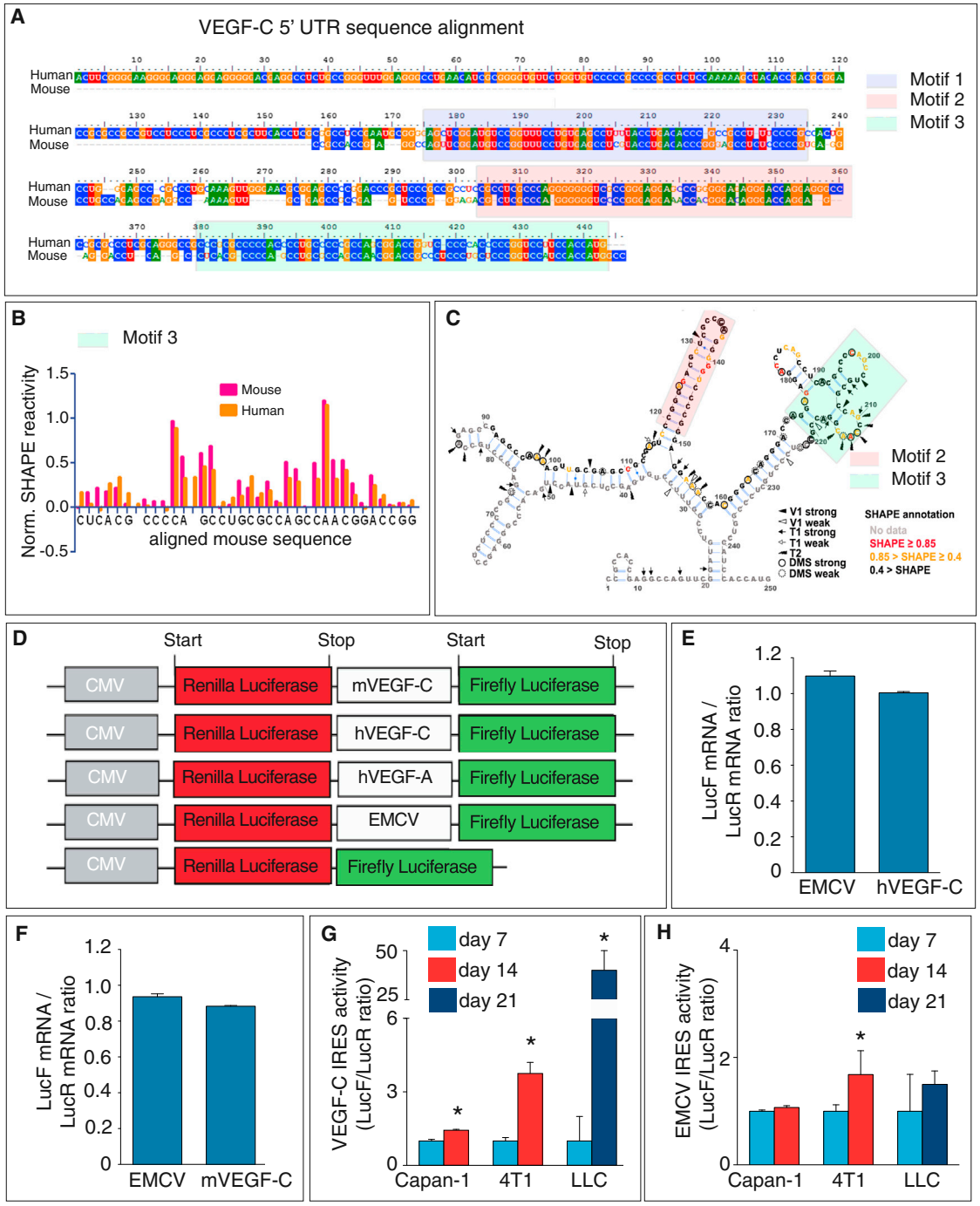

Figure 3. VEGF-C mRNA Contains an IRES Element Activated during Tumor Growth

(A) Sequence alignment of the murine and human VEGF-C 5′ UTR sequences. A color code is used for each nucleotide: guanine (orange), adenine (green), uridine (red), and cytosine (blue). Three stretches of nucleotides are highly conserved between the two RNA sequences: motif 1 (light blue), motif 2 (light orange), and motif 3 (light green).

(B) Quantification of the SHAPE analysis (see the Experimental Procedures) is shown for the conserved nucleotides of motif 3 of the human (orange) and murine (red) 5′ UTRs, showing very similar reactivity patterns.

(C) Putative secondary structure of the murine 5′ UTR of VEGF-C mRNA, as predicted on the basis of the ribose reactivities toward SHAPE and the reactivities of adenines at N1 and cytosines at N3 toward DMS. For each nucleotide, the level of reactivity toward SHAPE is indicated in red, yellow, or black font character for strong, medium, or weak reactivity, respectively. The cleavage sites induced by ribonucleases V1, T1, or T2 are indicated by arrows. Motifs 2 and 3 are color-coded as in (A).

(legend continued on next page)

secondary structure at single nucleotide resolution. SHAPE takes advantage of the fact that only flexible nucleotides are reactive toward hydroxyl-selective electrophiles, whereas constrained nucleotides are unreactive. We used as chemical probing reagents benzoyl cyanide in order to provide information on the flexibility of each ribose (Mortimer and Weeks, 2009) and dimethyl sulfate (DMS), which methylates single-stranded cytosines at N3 and adenines at N1 (Figure S2A). To footprint and probe the RNA structure, we also took advantage of the enzymatic cleavage by RNase T1 (which cleaves single-stranded RNA after unpaired guanines residues), RNase T2 (cleaving single-stranded RNA after unpaired nucleotides with a preference for adenines), and RNase V1 (cleaving base-paired nucleotide residues in a non-sequence-specific manner) (Figure S2A).

This analysis revealed that the 5′ UTRs were highly structured because of a high GC content (Figures 3A and 3B; Figures S2A and S2B). However, the concomitant presence of RNase V1 cleavages and of single-strand specific cuts, together with the sensitivity to modifications by DMS in the SHAPE analysis, suggested that these RNAs do not fold into a unique fixed structure but are able to adopt alternative conformations at equilibrium. Nevertheless, based on the quantification of the DMS and SHAPE reactivities, the most representative of the putative secondary structures of the murine 5′ UTR is shown in Figure 3C. Using sequence alignment, we observed three highly conserved regions between the human and murine 5′ UTRs (Figure 3A). Interestingly, SHAPE analysis revealed that two of these motifs adopted the same structure, since the reactivity pattern of the conserved residues was nearly identical (Figure 3B; Figure S2B). These motifs, located at the same distance from the initiation codon in human and murine RNAs, might be appropriate for binding of *trans*-acting factor(s) necessary to activate IRES-dependent translation.

The 5′ UTR of VEGF-C Exhibits IRES Activity

We then explored if the putative IRES sequences in the human and murine 5′ UTR of the VEGF-C mRNAs were translationally active and cloned these sequences in a double luciferase bicistronic vector (Figure 3D) (Créancier et al., 2000). In this vector, the first *Renilla* luciferase (LucR) cistron is translated by a cap-dependent mechanism, while the second firefly luciferase (LucF) cistron can be translated only if an IRES is present between the two cistrons. We used bicistronic vectors containing the encephalomyocarditis virus (EMCV) IRES sequence since it is not or only minimally regulated in mammalian cells, and we also used the VEGF-A IRES since it is activated by hypoxia (Bornes et al., 2007) (the VEGF-A data are discussed below). An empty control bicistronic vector, containing a sequence without IRES activity between the two cistrons, was inactive (Figure 3D; Figure S2C). Control RT-PCR analysis showed that both proteins were translated from a single mRNA transcript, since comparable amounts of LucR and LucF mRNA were measured (Figures 3E and 3F), indicating that a cryptic promoter or splicing event did not influence the results (Martineau et al., 2004).

To quantify the IRES activity in human and murine VEGF-C 5′ UTR sequences in vivo, Capan-1, 4T1, and LLC tumor cells were transduced with the bicistronic lentiviral vectors and injected subcutaneously (Capan-1, LLC) or orthotopically in the mammary fat pad (4T1). We used the human VEGF-C 5′ UTR for the human cell line (Capan-1) and the murine VEGF-C 5′ UTR for the murine cell lines (4T1, LLC). Transduction of the bicistronic vector did not affect tumor growth (Figures S2D and S2E). The VEGF-C IRES activity was quantified by measuring the LucF/LucR ratio as a parameter of the relative contribution of IRES-dependent versus cap-dependent translation after 7, 14, and 21 days. The IRES activity levels at day 14 and 21 were expressed relative to the IRES activity at day 7. These experiments revealed an IRES activity for both human and murine VEGF-C 5′ UTRs (Figures 3G and 3H). Furthermore, this IRES activity increased during tumor progression, especially in breast and lung tumors, while the EMCV IRES activity changed only minimally in 4T1 tumors (1.68-fold), e.g., less than the VEGF-C IRES activity in these tumors (3.75-fold).

The VEGF-C IRES Activity Is Higher in Metastatic Lymph Nodes

Analysis of the LYVE-1-positive lymphatic area in Capan-1, 4T1, and LLC tumors showed that lymphangiogenesis in lymph nodes was minimal at 3 days after inoculation but progressively increased from 7 days onward (Figures 4A–4J). This raised the question whether VEGF-C protein synthesis was increased in metastatic lymph nodes. However, substantial numbers of metastatic cytokeratin-positive tumor cells were detected in draining lymph nodes of Capan-1 and 4T1 tumors only from 14 days onward and of LLC tumors only from 21 days onward, i.e., later than the first signs of increased lymphangiogenesis in metastatic lymph nodes (Figures 4K–4N). Previous reports already documented that lymph node lymphangiogenesis precedes lymph node metastasis, presumably because primary tumors release VEGF-C in the lymph fluid of efferent lymphatics (Hirakawa, 2009).

We also explored whether tumor cells might upregulate VEGF-C production to higher levels, once they had intravasated and traveled through lymph vessels to the lymph node, and therefore analyzed the VEGF-C IRES activity in draining lymph nodes to which tumor cells metastasized. In order to compare the IRES activity in tumors and metastatic lymph nodes, the firefly/*Renilla* luciferase ratio in each tumor type was normalized

(D) Schematic representation of the bicistronic expression cassettes subcloned in lentivectors, encoding two luciferase reporters that are translated by cap-dependent translation (*Renilla* luciferase) or by IRES-dependent translation (firefly luciferase). IRESs used are the murine and human VEGF-C 5′ UTR, the human VEGF-A IRES, as well as the viral EMCV IRES (EMCV) and a short sequence devoid of IRES as positive and negative controls, respectively.
(E and F) mRNA expression analysis of firefly luciferase (LucF) and *Renilla* luciferase (LucR) by qRT-PCR on cells transduced with the bicistronic lentivector containing human (E) or murine (F) VEGF-C 5′ UTR, revealing comparable expression of LucR and LucF mRNA, suggesting transcription of a single mRNA (mean ± SEM; n = 6; p = NS).
(G and H) In vivo VEGF-C (G) and EMCV (H) IRES activity in Capan-1, 4T1, and LLC tumors (values are relative to day 7; mean ± SEM; n = 8–10; *p < 0.01).
See also Figure S2.

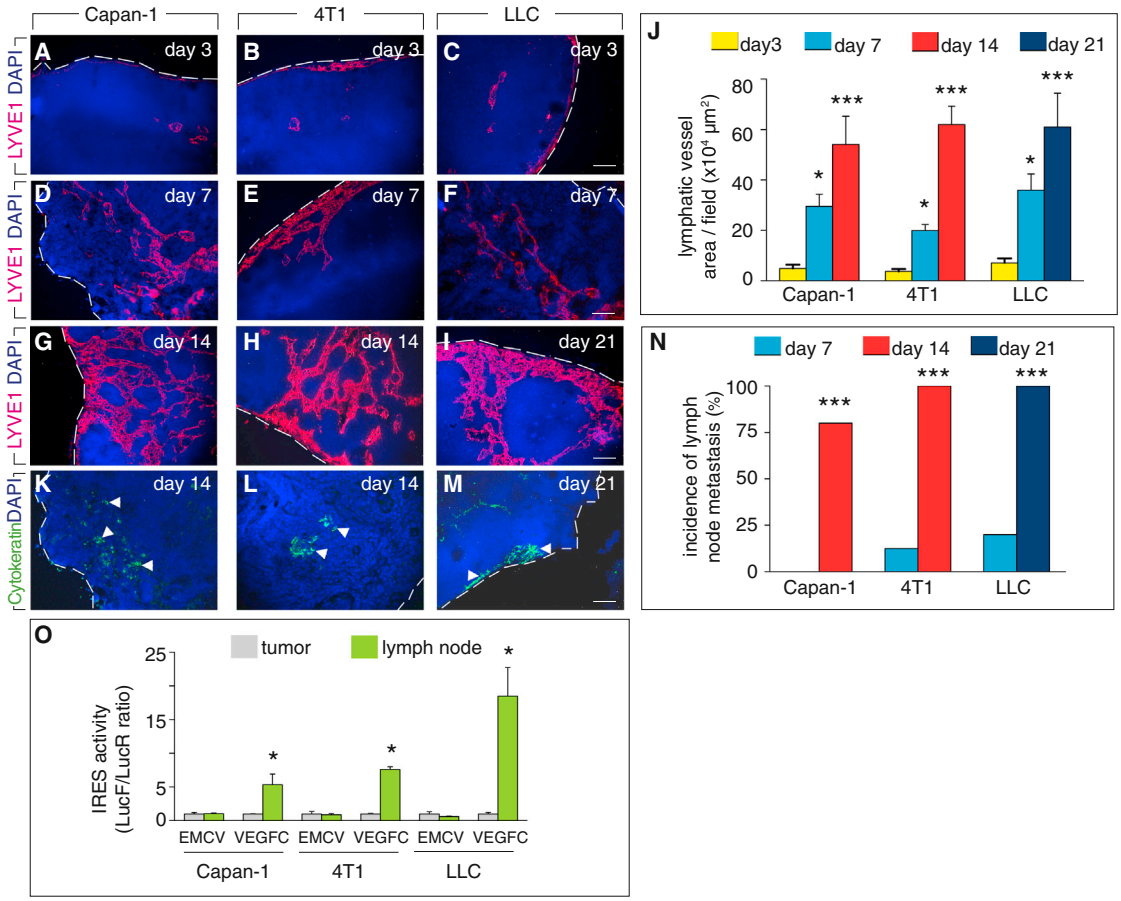

Figure 4. VEGF-C IRES Activity Is Higher in Metastatic Tumor Cells in the Lymph Node

(A–I) Staining for LYVE-1 (red) and nuclei (DAPI, blue) at day 3 (A–C), 7 (D–F) and 14 (G and H) or 21 (I) revealed that lymphangiogenesis progressively increased in tumor-draining lymph nodes in Capan-1, 4T1, and LLC tumors. Dashed lines denote the border of the tissue.

(J) Quantification of lymphatic vessel area in lymph node (mean ± SEM; n = 8–10; *p < 0.05, ***p < 0.001).

(K–M) Staining for cytokeratin (green, see arrowheads) and nuclei (DAPI, blue) revealed metastatic dissemination to lymph node of Capan-1, 4T1 and LLC tumors. Dashed lines denote the border of the tissue.

(N) Quantification of metastasis positive lymph nodes (mean ± SEM; n = 8–10; ***p < 0.001).

(O) In vivo VEGF-C- and EMCV-IRES activity in metastatic lymph nodes of Capan-1, 4T1, and LLC tumors at 14, 14, and 21 days, respectively (values are expressed relative to the respective value in the tumor; mean ± SEM; n = 8–10; *p < 0.01).

Scale bar represents 50 µm (all).

to the value of 1, both for the EMCV and VEGF-C IRES, and the IRES activities in the lymph nodes were expressed as a fold induction over the IRES activity in the tumor. This analysis revealed that compared to primary tumors, the VEGF-C IRES activity in metastatic lymph nodes was 5-, 7-, and 18-fold higher in the Capan-1, 4T1, and LLC tumor models at 14, 14, and 21 days after tumor inoculation, respectively, while the EMCV IRES activity was not affected (Figure 4O). These findings suggested that the lymphatic milieu influenced VEGF-C translation in tumor cells.

Lymph Vessels Are Hypoxic and Develop Nearby Hypoxic Tumor Cells

We then sought to determine why the lymphatic milieu enhanced the VEGF-C IRES activity in metastatic tumor cells. Since lymphatics are known to be hypoxic (Guzy et al., 2008; Ivanovic, 2009) and IRES elements are activated in cellular stress conditions such as hypoxia (Braunstein et al., 2007; Komar and Hatzoglou, 2011; Pestova et al., 2001; Sachs, 2000; Silvera and Schneider, 2009; Spriggs et al., 2010; Vagner et al., 2001), we explored whether hypoxia affected IRES-dependent initiation of translation of VEGF-C. We first explored a possible link between hypoxia and lymphatic development and therefore double stained tumors for the hypoxyprobe pimonidazole and the lymphatic markers LYVE-1 or podoplanin. Already at an early stage of tumor development (in <5 mm^3 tumors), the pancreas, breast, and lung cancer models contained hypoxic regions, which became more widespread and stained more strongly after 2 weeks (Figures 5A–5C). Immunoblotting for HIF-1α confirmed activation of this hypoxia-inducible transcription factor (Figure 5D). In all cancer models, lymph vessels developed in proximity of hypoxic tumor cell clusters (Figures 5E–5G). Unlike blood

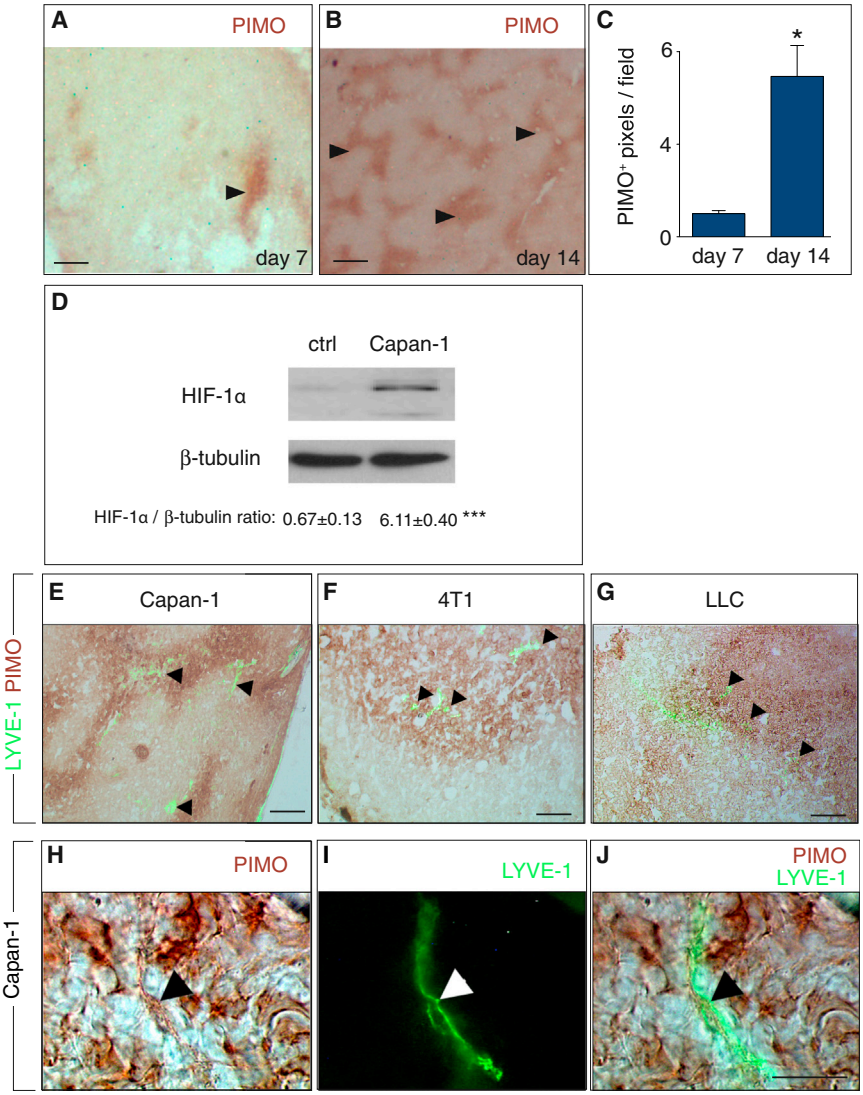

Figure 5. Tumor VEGF-C Levels Are Increased in Hypoxic Zones

(A–C) Immunodetection of hypoxic areas (hypoxyprobe, brown) in Capan-1 tumors revealed few small hypoxic areas at early time points (A, day 7), which became more abundant by 14 days after injection (B). Arrowheads indicate pimonidazole adduct (PIMO)-positive hypoxic areas. Quantification of $PIMO^+$ area is shown in (C) (mean ± SEM; n = 10; *p < 0.001).

(D) Immunoblot for HIF-1α in Capan-1 tumors showing stabilization of the protein in vivo. Normal healthy skin was used as control. Densitometric quantification is shown (mean ± SEM; n = 6; ***p < 0.001). ctrl, control.

(E–G) Staining for LYVE-1 (green, see arrowheads) revealing the presence of lymphatic vessels close to hypoxic areas (hypoxyprobe [PIMO], brown) in Capan-1 (E), 4T1 (F), and LLC (G) tumors.

(H–J) Staining of Capan-1 tumor for LYVE-1 (green, arrowhead) and hypoxyprobe (PIMO, brown) revealed hypoxic lymph vessels. Merged image is shown in (J).

Scale bar represents 50 μm (A and B), 50 μm (E–G), 25 μm H–J). See also Figure S3.

endothelial cells, lymphatic endothelial cells also stained positively for pimonidazole, indicating that lymph vessels are hypoxic (Figures 5H–5J; Figures S3A–S3F).

Hypoxia Induces VEGF-C Expression by a Nontranscriptional Mechanism

We then studied the regulation of IRES-dependent VEGF-C translation by hypoxia. Immunostaining revealed that VEGF-C and LucF were expressed predominantly in pimonidazole-positive hypoxic tumor areas in vivo (Figures 6A–6F). To study the effect of hypoxia on VEGF-C expression in vitro, we exposed LLC, Capan-1, or 4T1 tumor cells to 1% oxygen or to cobalt chloride ($CoCl_2$), known to activate hypoxia signaling. Hypoxia reduced VEGF-C mRNA levels in LLC and 4T1 cells while not affecting its levels in Capan-1 cells (Figures 6G–6I). In LLC and 4T1 cells, hypoxia increased the protein levels of VEGF-C and of hypophosphorylated 4E-BP1, suggesting increased VEGF-C production despite a decrease in cap-dependent initiation of translation (Figures 6J and 6K). In Capan-1 cells, VEGF-C protein levels were comparable in hypoxic conditions, though 4E-BP1 dephosphorylation was increased, suggesting that the reduced cap-dependent initiation of VEGF-C translation was balanced off by an increase in IRES-dependent initiation of VEGF-C translation (Figures 6J and 6K). In each cell line, eIF2α phosphorylation was increased by hypoxia, suggesting that hypoxia downregulated global mRNA translation (Figures 6J and 6K). Since hypoxia increased the VEGF-C IRES activity in all human and murine tumor lines (also in the Capan-1 cells, in which VEGF-C levels did not increase) (Figures 6L–6N), hypoxia thus induced a switch from cap-dependent to IRES-dependent initiation of VEGF-C translation. Similar results were obtained when we used $CoCl_2$ (Figure 6O). Phosphorylation of eIF2α inhibits the EMCV IRES activity (Sanz et al., 2013) and the increased eIF2α phosphorylation levels might thus be responsible for the inhibition of the EMCV IRES activity in hypoxia, while the variable EMCV IRES activity in hypoxia in distinct tumor cell lines likely reflects cell-type-dependent regulation of this IRES activity, which has been recognized previously (Pilipenko et al., 2000).

The VEGF-C IRES Activity Is Reduced in More Oxygenated Tumors

We then explored whether tumor oxygen levels in vivo influenced the switch between cap-dependent VEGF-C translation (in oxygenated conditions) versus IRES-dependent VEGF-C translation (in hypoxic conditions). We therefore used prolyl

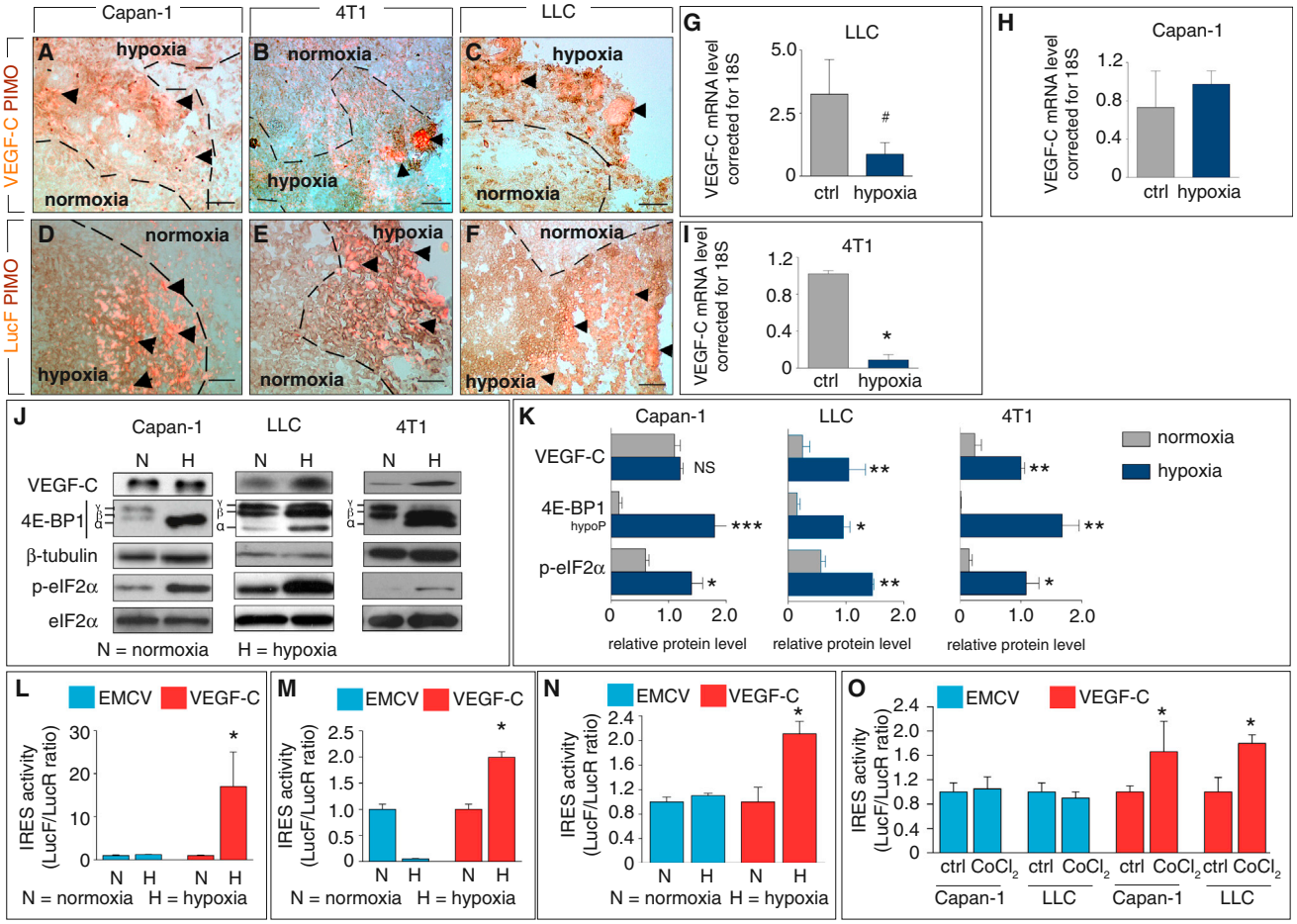

Figure 6. Hypoxia Induces VEGF-C-IRES Activity In Vitro

(A–C) Staining for VEGF-C (red) and hypoxyprobe (PIMO, brown) revealed VEGF-C colocalization (arrows) in hypoxic areas in Capan-1 (A), 4T1 (B), and LLC (C) tumors. Dashed lines denote more hypoxic from more normoxic zones.

(D–F) Staining for firefly luciferase (LucF, red) and hypoxyprobe (PIMO, brown) revealed IRES-dependent luciferase translation (arrows) primarily in hypoxic areas in Capan-1 (D), 4T1 (E), and LLC (F) tumors. Dashed lines denote more hypoxic from more normoxic zones.

(G–I) qRT-PCR for VEGF-C showing reduced mRNA levels in hypoxic conditions in LLC (G) and 4T1 (I) tumor cells, but not in Capan-1 tumor cells (H) (mean ± SEM; n = 9, *p < 0.001 in I; #p = 0.059 in G; p = NS in H).

(J and K) Immunoblot of VEGF-C, 4E-BP1, eIF2α, and phosphorylated eIF2α (p-eIF2α) in Capan-1, LLC, or 4T1 tumor cells, cultured in normoxia or hypoxia (1% O_2). Quantification by densitometry is shown in (K). Relative levels are normalized to β-tubulin (VEGF-C, hypophosphorylated 4E-BP1) or to eiF2α (p-eiF2α) (mean ± SEM; n = 3–6; *p < 0.05, **p < 0.01).

(L–N) VEGF-C- and EMCV IRES activity under normoxic and hypoxic conditions (1% O_2) in Capan-1 (L), 4T1 (M), and LLC (N) tumor cells in vitro (values are expressed relative to the respective normoxia condition; mean ± SEM; n = 6; *p < 0.01 versus normoxia).

(O) VEGF-C- and EMCV IRES activity in control and $CoCl_2$ conditions in Capan-1 and LLC cells in vitro (values are expressed relative to the respective controls; mean ± SEM; n = 5; *p < 0.01).

Scale bar represents 50 μm (A–F). ctrl, control.

hydroxylase domain protein-2 $(PHD2)^{+/-}$ mice, in which tumor hypoxia is reduced because of normalization of tumor blood vessels and improved tumor vessel perfusion (Mazzone et al., 2009), hypothesizing that the VEGF-C IRES activity would be reduced in these mice. We thus implanted bicistronic luciferase vector-transduced LCC tumor cells in wild-type (WT) and $PHD2^{+/-}$ mice. Tumor growth of cancer cells, transduced with VEGF-C- or EMCV-IRES vectors, was comparable in WT and $PHD2^{+/-}$ mice (Figure S4A), consistent with reports that PHD2 haplodeficiency did not affect tumor growth (Mazzone et al., 2009). Also, staining for the hypoxia marker pimonidazole demonstrated that hypoxia levels were lower in EMCV IRES- and VEGF-C IRES-expressing tumors in $PHD2^{+/-}$ mice than in WT mice (Figures 7A, 7D, and 7G).

Compared to tumors in WT mice, tumors in $PHD2^{+/-}$ mice had similar VEGF-C immunoreactive protein levels, which colocalized in part with the pimonidazole-positive hypoxic regions, showing that both normoxic and hypoxic tumor cells produced VEGF-C (Figures 7B, 7C, 7E, 7F, and 7H). Immunoblotting confirmed these findings (Figure S4B). However, a reduced fraction of

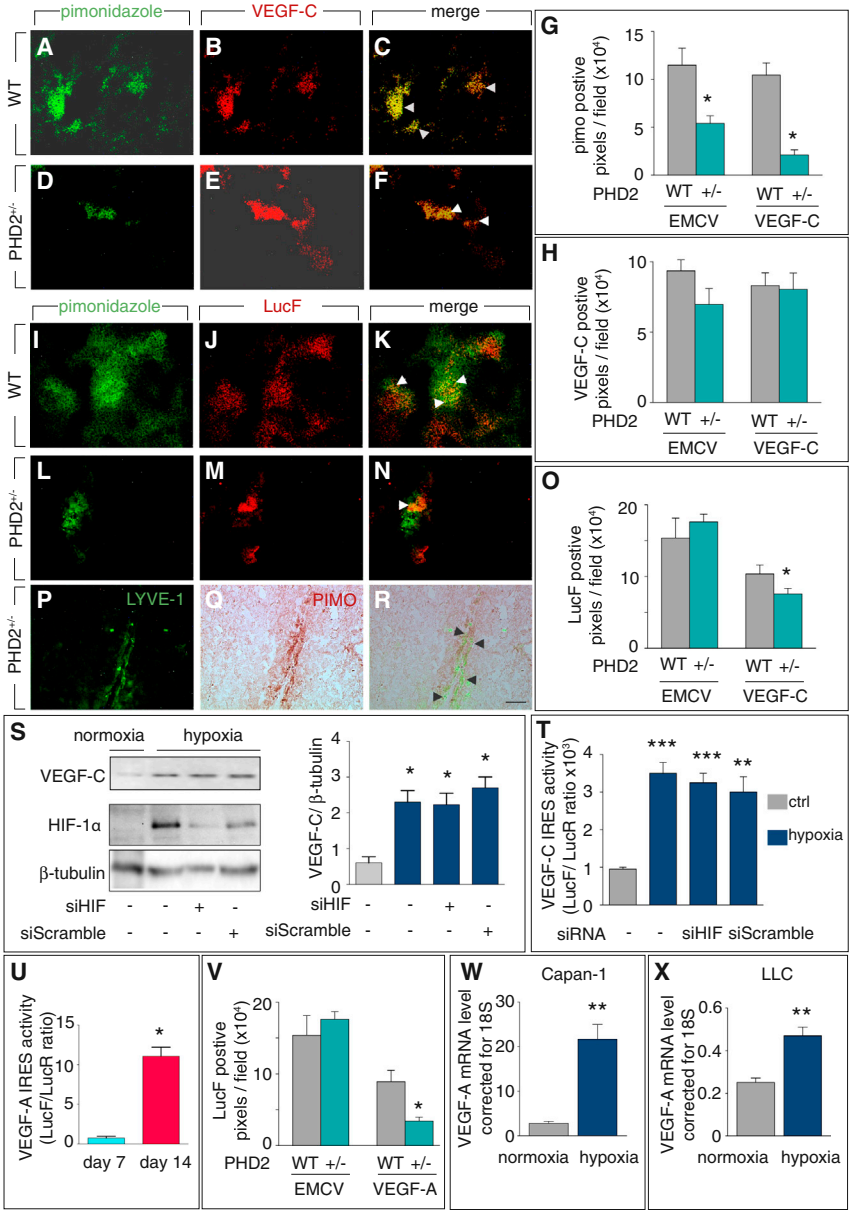

Figure 7. VEGF-C Induction by Hypoxia Is Translationally Regulated but HIF-1α Independent

(A–F) Immunostaining for hypoxyprobe (pimonidazole, green) and VEGF-C (red) in LLC tumors in wild-type (WT) (A–C) and PHD2$^{+/-}$ mice (D–F).

(G) Quantification of pimonidazole-positive pixel density in tumors transduced with EMCV- or VEGF-C IRES luciferase constructs showed a decrease in hypoxia in PHD2$^{+/-}$ mice (mean ± SEM; n = 6; *p < 0.05).

(H) Quantification of VEGF-C-positive pixel density in tumors transduced with EMCV- or VEGF-C IRES luciferase lentivector constructs revealing no differences (mean ± SEM; n = 8–10; p = NS).

(I–O) Staining for firefly luciferase (LucF, red) and hypoxyprobe (pimonidazole, green) revealed reduced VEGF-C IRES-dependent translation in LLC-bearing PHD2$^{+/-}$ mice (L–N) as compared to WT mice (I–K). Quantification of LucF-positive pixel density is shown in (O) confirming the decrease in luciferase signal for VEGF-C-IRES, which was not seen with the EMCV control IRES (mean ± SEM; n = 8–10; *p < 0.01).

(P–R) Micrographs of LLC tumor sections in PHD2$^{+/-}$ mice, stained for LYVE-1 (green) and hypoxyprobe (PIMO, brown), revealing that lymph vessels were hypoxic in this model.

(S) Immunoblot of VEGF-C or HIF-1α in lysates of Capan-1 cells incubated in normoxia or hypoxia and treated with or without siRNA against HIF-1α (siHIF) or a scrambled siRNA control (siScramble). Densitometric quantification is shown in the graph (right) (mean ± SEM; n = 4; *p < 0.01).

(T) VEGF-C IRES activity in Capan-1 cell lines in vitro incubated under normoxia or hypoxia and treated with or without siRNA against HIF-1α or a scrambled siRNA control (mean ± SEM; n = 5; ***p < 0.001).

(U) VEGF-A IRES activity in Capan-1 tumors in vivo revealing increased IRES activity with tumor progression (mean ± SEM; n = 8–10; *p < 0.005).

(V) Quantification of staining for firefly luciferase (LucF) revealed that VEGF-A IRES activity was lower in LLC tumors in PHD2$^{+/-}$ mice than in WT mice. The activity of EMCV IRES was not affected (mean ± SEM; n = 6; *p < 0.01). Note: since the data shown in Figure 7V and Figure 7O were generated in the same experiments, the EMCV control data are the same.

(W and X) qRT-PCR for VEGF-A showing increased mRNA levels in hypoxic conditions in Capan-1 (C) and LLC (D) tumor cells in vitro (mean ± SEM; n = 6; *p < 0.05).

Scale bar represents 50 μm (all). See also Figure S4.

VEGF-C was translated via IRES-dependent mechanisms in the more oxygenated tumors of PHD2$^{+/-}$ mice. Indeed, when double staining for pimonidazole and firefly luciferase (LucF), VEGF-C IRES-expressing tumors in PHD2$^{+/-}$ mice had reduced LucF but increased LucR levels (Figures 7I–7O; Figures S4C and S4D), indicating that the VEGF-C IRES activity was reduced while cap-dependent translation initiation was increased. VEGF-C IRES-dependent translation of LucF was only detected in the residual hypoxic tumor zones in PHD2$^{+/-}$ mice (Figures 7L–7N). Interestingly, even though overall tumor oxygenation in PHD2$^{+/-}$ mice was improved because of blood vessel normalization, lymph vessels remained immunoreactive for the hypoxyprobe pimonidazole in tumors of PHD2$^{+/-}$ mice (Figures 7P–7R). Thus, IRES-dependent VEGF-C translation was reduced in more oxygenated tumors of PHD2$^{+/-}$ mice, confirming the regulation of the translational switch (cap versus IRES dependence) by oxygen levels in vivo. That VEGF-C protein levels were not lower in tumors of PHD2$^{+/-}$ mice than in WT mice, despite overall improved oxygenation, may be due to the fact that the oxygenation conditions in tumors of PHD2$^{+/-}$ mice were still not sufficiently improved to completely abrogate IRES-dependent VEGF-C translation. In addition, even though HIF-1α levels are

reduced in more oxygenated tumors of PHD2$^{+/-}$ mice (Mazzone et al., 2009), the residual HIF-1α levels may still promote cap-dependent translation, since HIF-1α induces the transcription of the cap-binding factor eIF-4E (Yi et al., 2013).

HIF-1α-Independent Hypoxic Induction of VEGF-C Synthesis

To explore if VEGF-C protein production in hypoxic conditions was HIF dependent, we used a small interfering RNA (siRNA) against human HIF-1α (siHIF) to silence HIF-1α expression, which reduced HIF-1α protein levels to nearly undetectable levels in hypoxic Capan-1 tumor cells (Figure 7S). Silencing of HIF-1α also reduced the expression levels of VEGF-A, phosphoglycerate kinase (PGK), hexokinase-2, and the glucose transporter GLUT-1, all known HIF-1α target genes (Figure S4E). Despite the strong decrease of the HIF-1α levels in hypoxic Capan-1 tumor cells transfected with siHIF (Figure 7S), VEGF-C protein levels were maintained in hypoxic conditions (Figure 7S), whereas the VEGF-C IRES activity was not affected by HIF-1α silencing (Figure 7T). Thus, these data suggest that the posttranscriptional induction of VEGF-C via IRES was independent of HIF-1α.

Regulation of VEGF-A Expression by Hypoxia

For reasons of comparison, we also studied the relative importance of the cap-dependent versus IRES-dependent translation of VEGF-A in hypoxia. Previous in vitro studies documented that VEGF-A translation relies on cap-dependent mechanisms in normoxia and on IRES-dependent mechanisms in hypoxia (Bornes et al., 2004). Transgenic mouse lines, expressing reporter genes under the control of IRESs, also revealed that VEGF-A translation in ischemic muscle partly depends on the IRES activity (Bornes et al., 2007). However, it is unknown whether IRES-dependent translation of VEGF-A can also occur in tumors or metastatic lymph nodes. When tumor cells, stably transduced with a bicistronic lentiviral vector containing the VEGF-A IRES sequence, were injected in vivo, the VEGF-A IRES activity levels were detectable and increased during tumor progression (Figure 7U). The VEGF-A IRES activity was sensitive to oxygen levels in tumors in vivo, since tumors (transduced with lentiviral bicistronic vectors containing VEGF-A IRES) had lower VEGF-A IRES activity levels in PHD2$^{+/-}$ mice, as revealed by staining for firefly luciferase (Figure 7V). This was not influenced by the tumor size, since tumor growth was not affected by the PHD2 genotype or type of bicistronic vector (VEGF-A- or EMCV-IRES) (Figure S4F).

However, different from VEGF-C, regulation of VEGF-A expression also relied on transcriptional upregulation in hypoxic conditions. Indeed, VEGF-A mRNA levels were increased in tumor cells in hypoxia (Figures 7W and 7X) and also increased during tumor progression in vivo, both at the protein and mRNA levels (Figures S4G–S4J). Thus, unlike VEGF-A, the expression of which is upregulated in hypoxia at the transcriptional and translational level, the expression of VEGF-C in hypoxia is regulated by translational, but not by transcriptional, mechanisms.

DISCUSSION

We identified a translational regulation of VEGF-C production in hypoxic conditions, both in primary tumors and in (pre)-metastatic lymph nodes, that is distinct from previously identified mechanisms of how hypoxia stimulates lymphangiogenesis.

Tumor Cells Metastasizing via Hypoxic Lymphatics Induce VEGF-C

For tumor cells to spread to distant organs via lymphatics, they induce lymphangiogenesis. However, since tumors are often deprived of oxygen and lymphatics are extremely hypoxic (Guzy et al., 2008; Ivanovic, 2009), tumor cells must have mechanisms to stimulate lymph vessel growth in hypoxic conditions. Our findings demonstrate that tumor cells can upregulate VEGF-C protein levels in hypoxic conditions in vitro and in vivo and that lymph vessels grew in and around hypoxic tumor areas, where VEGF-C was produced. While hypoxia often upregulates protein levels via HIF-1α-dependent gene transcription, this study shows that hypoxia augments VEGF-C protein levels via a HIF-1α-independent effect on VEGF-C IRES-dependent initiation of translation.

Hypoxia Regulates VEGF-C Protein Levels via an IRES-Dependent Activity

We demonstrate that murine and human VEGF-C mRNAs are translated by IRES-dependent initiation of translation in hypoxic tumor areas during tumor development in vivo. Sequence alignment revealed that murine and human VEGF-C 5′ UTRs share three highly conserved motifs. Interestingly, probing the RNA secondary structures by SHAPE analysis showed that two of these motifs adopt the same two-dimensional structure, since the reactivity pattern of the conserved residues was nearly identical. These motifs, located at the same distance from the initiation codon, might be appropriate for binding of specific *trans*-acting factor(s), necessary to activate IRES-dependent translation. Use of a bicistronic vector provided functional evidence that the 5′ UTR of murine and human VEGF-C mRNA indeed functioned as IRES sequences to initiate cap-independent translation of the VEGF-C mRNA. Thus, translation of the VEGF-C mRNA in normoxia occurs via cap- and/or IRES-dependent mechanisms. In hypoxia, when global translation is suppressed through dephosphorylation of 4E-BP1 and increased phosphorylation of eIF2α, IRES-mediated mRNA translation is activated, leading to an overall increase in VEGF-C protein levels.

VEGF-C IRES Activity Is Higher in Lymph Nodes

Previous studies reported that expression of VEGF-C by cancer cells promotes tumor and lymph node lymphangiogenesis as well as metastasis (Hirakawa et al., 2005, 2007). Even before metastatic tumor cells reach the sentinel lymph nodes, VEGF-C, released by malignant cells of the primary tumor into the lymphatic circulation, stimulates lymphangiogenesis in lymph nodes at a distance (Hirakawa et al., 2005, 2007). Using luciferase reporters of posttranscriptional VEGF-C regulation, we observed that the VEGF-C IRES firefly luciferase activity was increased in lymph nodes at the time when they were colonized by metastatic tumor cells. Notably, however, the induction of the VEGF-C IRES activity was higher in tumor cells that had metastasized to the lymph nodes than in tumor cells that were present in the primary tumors. Lymphangiogenesis was also

more extensive in metastatic lymph nodes than in primary tumors. These data indicate that the lymph node milieu stimulates VEGF-C expression. Since lymphatics are highly hypoxic, the hypoxic milieu seems to be of key importance to activate IRES-dependent VEGF-C translation.

HIF-1α-Independent Regulation of VEGF-C Translation in Hypoxia

Hypoxia signaling is well known to stimulate angiogenesis, in part by promoting HIF-1α dependent transcription of VEGF-A as well as by stimulating IRES-dependent VEGF-A translation (Bornes et al., 2007; Huez et al., 2001). In contrast, VEGF-C transcript levels were reduced, yet VEGF-C protein levels were increased, in hypoxia by switching from cap-dependent to IRES-dependent VEGF-C translation. Notably, this regulation seemed to be independent of HIF-1α, since near-complete silencing of HIF-1α to levels sufficient to lower HIF-1α target gene transcription did not abrogate the hypoxia-induced post-transcriptional IRES-activated translation of VEGF-C mRNA and production of VEGF-C protein. Different molecular mechanisms thus evolved to ensure production of VEGF-A and VEGF-C, two closely related and homologous members of the VEGF family.

Hypoxic Lymph Vessels Ensure Lymphangiogenesis in Cancer

Our findings may also be relevant to understand how tumor cells have developed mechanisms to ensure spreading via lymphatics in oxygen-deprived conditions. Lymph vessels are severely hypoxic, not only because they lack oxygen-carrying red blood cells, but also because they reside in very hypoxic regions in tissues and tumors (Guzy et al., 2008; Ivanovic, 2009). Such a hypoxic milieu suppresses cap-dependent mRNA translation of VEGF-C in tumor cells, traveling inside lymphatics to the lymph nodes. However, by switching to IRES-dependent initiation of translation of VEGF-C, tumor cells can upregulate the production of this key lymphangiogenic factor in hypoxia and thereby ensure increased growth of lymph vessels via which they metastasize. Hence, tumor cells have adopted mechanisms to stimulate lymphangiogenesis when metastasizing through hypoxic lymph vessels and lymph nodes.

EXPERIMENTAL PROCEDURES

All human tissue was used under approval from the Human Subjects Institutional Review Board of the University of Toulouse III. More detailed procedures are described in Supplemental Experimental Procedures.

Tissue Specimens

In total, 15 primary human breast cancer specimens and their associated lymph nodes were collected from pretreatment surgical resections (Rangueil Hospital, Toulouse, France). Sample collection was approved by the INSERM Institutional Review Board (DC-2008-463) and Research State Department (Ministère de la Recherche, ARS, CPP2, authorization AC-2008-820).

Cell Culture

Cell culture of Capan-1 pancreatic carcinoma cells, 4T1 breast carcinoma, and LLC cells under normoxia or hypoxia (1% O_2 or 300 μM $CoCl_2$) was as described in the Supplemental Experimental Procedures.

Tumor Studies and Immunohistochemical Phenotyping

Animal experiments were conducted in accordance with recommendations of the European Convention for the Protection of Vertebrate Animals used for experimentation and according to the INSERM IACUC (France) and the KU Leuven (Belgium) guidelines for laboratory animal husbandry. All animal experiments were approved by the local branch Inserm Rangueil-Purpan of the Midi-Pyrénées ethics committee, France (protocol 091037615), or by the Institutional Animal Care and Research Advisory Committee of the KU Leuven, Leuven, Belgium (protocol P166/2011). The LLC syngenic tumor model in C57Bl6 mice, Capan-1 xenograft model in NMRI nude mice, syngenic orthotopic 4T1 breast carcinoma model in Balb/c mice, and the collection and immunohistological analysis of tumor and lymph nodes was performed as detailed in the Supplemental Experimental Procedures.

RNA and Protein Analysis

SHAPE Analysis

In-vitro-transcribed RNA was prepared and subjected to SHAPE analysis as previously described (Helfer et al., 2013) (Mortimer and Weeks, 2009) and further detailed in the Supplemental Experimental Procedures.

RNA Analysis

Expression of human and murine VEGF-C, VEGF-A, hexokinase II, Glut1, PGK, LucR, and LucF was by SYBR green quantitative RT-PCR (Table S1) as described in the Supplemental Experimental Procedures.

Protein Analysis

VEGF-C protein levels in Capan-1 tumor extracts were measured by ELISA (R&D Systems).

Lentivector Construction and Luciferase Reporter Gene Assay

Cloning of the cDNAs coding human and murine VEGF-C 5′ UTR, VEGF-A 5′ UTR, and EMCV 5′ UTR into the bicistronic lentivectors expressing *Renilla* luciferase under the cytomegalovirus promoter and firefly luciferase under the control of the respective 5′ UTR IRES, and cell transduction was as described in the Supplemental Experimental Procedures. In vitro or ex vivo luciferase assays on cell or tissue lysates were performed using the Dual-Luciferase Assay System kit (Promega).

siRNA and Cell Transfection

siRNA-mediated silencing of human HIF1α was done using a pool of siRNAs as listed in the Supplemental Experimental Procedures. Transfection of Capan-1 cells and verification of silencing by immunoblotting was as described in the Supplemental Experimental Procedures.

Statistical Analysis

All statistical analyses were performed with a two-tailed Student's t test or one-way ANOVA. All experiments were performed three times, with one exception, where the incidence of metastasis is reported as the average ± SEM of three separate animal experiments. All other data presented are of one representative experiment.

SUPPLEMENTAL INFORMATION

Supplemental Information includes Supplemental Experimental Procedures, four figures, and one table and can be found with this article online at http://dx.doi.org/10.1016/j.celrep.2013.12.011.

ACKNOWLEDGMENTS

This study was supported by the Ligue Régionale Contre le Cancer, Fondation pour la Recherche Médicale and Association Française contre les Myopathies, Association pour la Recherche sur le Cancer, and Conseil Régional Midi-Pyrénées (France). We thank the Biological Resources Center and G. Escourrou and I. Rouquette from the Pathology and Histology Department of Rangueil Hospital in Toulouse for providing human tissue samples. We thank J.J. Maoret (GeT Genotoul Platform), Y. Barreira (ANEXPLO Genotoul Platform), A. Delluc-Clavières, and L. Van den Berghe for technical assistance and F. Lenfant, H. Prats, and P. Romby for scientific support. A.K. is funded

by a fellowship of the Belgian Science Fund—Flanders; F.H. is funded by the Conseil Régional Midi-Pyrénées (France). The work of P.C. is funded by Long-term Structural Funding Methusalem by the Flemish Government, the Interuniversitary Actraction Poles (P7/03), the Belgian Government, and Leducq Transatlantic Network—Artemis.

Received: May 24, 2013
Revised: October 28, 2013
Accepted: December 6, 2013
Published: January 2, 2014

REFERENCES

Albrecht, I., and Christofori, G. (2011). Molecular mechanisms of lymphangiogenesis in development and cancer. Int. J. Dev. Biol. *55*, 483–494.

Alitalo, K. (2011). The lymphatic vasculature in disease. Nat. Med. *17*, 1371–1380.

Alitalo, A., and Detmar, M. (2012). Interaction of tumor cells and lymphatic vessels in cancer progression. Oncogene *31*, 4499–4508.

Bonnal, S., Schaeffer, C., Créancier, L., Clamens, S., Moine, H., Prats, A.C., and Vagner, S. (2003). A single internal ribosome entry site containing a G quartet RNA structure drives fibroblast growth factor 2 gene expression at four alternative translation initiation codons. J. Biol. Chem. *278*, 39330–39336.

Bornes, S., Boulard, M., Hieblot, C., Zanibellato, C., Iacovoni, J.S., Prats, H., and Touriol, C. (2004). Control of the vascular endothelial growth factor internal ribosome entry site (IRES) activity and translation initiation by alternatively spliced coding sequences. J. Biol. Chem. *279*, 18717–18726.

Bornes, S., Prado-Lourenco, L., Bastide, A., Zanibellato, C., Iacovoni, J.S., Lacazette, E., Prats, A.C., Touriol, C., and Prats, H. (2007). Translational induction of VEGF internal ribosome entry site elements during the early response to ischemic stress. Circ. Res. *100*, 305–308.

Braunstein, S., Karpisheva, K., Pola, C., Goldberg, J., Hochman, T., Yee, H., Cangiarella, J., Arju, R., Formenti, S.C., and Schneider, R.J. (2007). A hypoxia-controlled cap-dependent to cap-independent translation switch in breast cancer. Mol. Cell *28*, 501–512.

Bushell, M., Stoneley, M., Sarnow, P., and Willis, A.E. (2004). Translation inhibition during the induction of apoptosis: RNA or protein degradation? Biochem. Soc. Trans. *32*, 606–610.

Christiansen, A., and Detmar, M. (2011). Lymphangiogenesis and cancer. Genes Cancer *2*, 1146–1158.

Créancier, L., Morello, D., Mercier, P., and Prats, A.C. (2000). Fibroblast growth factor 2 internal ribosome entry site (IRES) activity ex vivo and in transgenic mice reveals a stringent tissue-specific regulation. J. Cell Biol. *150*, 275–281.

Deer, E.L., González-Hernández, J., Coursen, J.D., Shea, J.E., Ngatia, J., Scaife, C.L., Firpo, M.A., and Mulvihill, S.J. (2010). Phenotype and genotype of pancreatic cancer cell lines. Pancreas *39*, 425–435.

Garmy-Susini, B., Avraamides, C.J., Schmid, M.C., Foubert, P., Ellies, L.G., Barnes, L., Feral, C., Papayannopoulou, T., Lowy, A., Blair, S.L., et al. (2010). Integrin alpha4beta1 signaling is required for lymphangiogenesis and tumor metastasis. Cancer Res. *70*, 3042–3051.

Guzy, R.D., Sharma, B., Bell, E., Chandel, N.S., and Schumacker, P.T. (2008). Loss of the SdhB, but Not the SdhA, subunit of complex II triggers reactive oxygen species-dependent hypoxia-inducible factor activation and tumorigenesis. Mol. Cell. Biol. *28*, 718–731.

Helfer, A.C., Romilly, C., Chevalier, C., Lioliou, E., Marzi, S., and Romby, P. (2013). Probing RNA Structure. In Vitro with Enzymes and Chemicals, *Volume 2*, Second Edition (Weinheim: Wiley-VCH Verlag).

Hirakawa, S. (2009). From tumor lymphangiogenesis to lymphvascular niche. Cancer Sci. *100*, 983–989.

Hirakawa, S., Kodama, S., Kunstfeld, R., Kajiya, K., Brown, L.F., and Detmar, M. (2005). VEGF-A induces tumor and sentinel lymph node lymphangiogenesis and promotes lymphatic metastasis. J. Exp. Med. *201*, 1089–1099.

Hirakawa, S., Brown, L.F., Kodama, S., Paavonen, K., Alitalo, K., and Detmar, M. (2007). VEGF-C-induced lymphangiogenesis in sentinel lymph nodes promotes tumor metastasis to distant sites. Blood *109*, 1010–1017.

Huez, I., Bornes, S., Bresson, D., Créancier, L., and Prats, H. (2001). New vascular endothelial growth factor isoform generated by internal ribosome entry site-driven CUG translation initiation. Mol. Endocrinol. *15*, 2197–2210.

Ivanovic, Z. (2009). Physiological, ex vivo cell oxygenation is necessary for a true insight into cytokine biology. Eur. Cytokine Netw. *20*, 7–9.

Kaelin, W.G., Jr., and Ratcliffe, P.J. (2008). Oxygen sensing by metazoans: the central role of the HIF hydroxylase pathway. Mol. Cell *30*, 393–402.

Komar, A.A., and Hatzoglou, M. (2011). Cellular IRES-mediated translation: the war of ITAFs in pathophysiological states. Cell Cycle *10*, 229–240.

Koumenis, C., and Wouters, B.G. (2006). "Translating" tumor hypoxia: unfolded protein response (UPR)-dependent and UPR-independent pathways. Mol. Cancer Res. *4*, 423–436.

Larsson, O., Tian, B., and Sonenberg, N. (2013). Toward a genome-wide landscape of translational control. Cold Spring Harb. Perspect. Biol. *5*, a012302.

Liang, X., Yang, D., Hu, J., Hao, X., Gao, J., and Mao, Z. (2008). Hypoxia inducible factor-alpha expression correlates with vascular endothelial growth factor-C expression and lymphangiogenesis/angiogenesis in oral squamous cell carcinoma. Anticancer Res. *28* (3A), 1659–1666.

Majmundar, A.J., Wong, W.J., and Simon, M.C. (2010). Hypoxia-inducible factors and the response to hypoxic stress. Mol. Cell *40*, 294–309.

Martineau, Y., Le Bec, C., Monbrun, L., Allo, V., Chiu, I.M., Danos, O., Moine, H., Prats, H., and Prats, A.C. (2004). Internal ribosome entry site structural motifs conserved among mammalian fibroblast growth factor 1 alternatively spliced mRNAs. Mol. Cell. Biol. *24*, 7622–7635.

Martineau, Y., Azar, R., Bousquet, C., and Pyronnet, S. (2013). Anti-oncogenic potential of the eIF4E-binding proteins. Oncogene *32*, 671–677.

Martinez-Corral, I., and Makinen, T. (2013). Regulation of lymphatic vascular morphogenesis: Implications for pathological (tumor) lymphangiogenesis. Exp. Cell Res. http://dx.doi.org/10.1016/j.yexcr.2013.01.016

Maxwell, P.H. (2005). The HIF pathway in cancer. Semin. Cell Dev. Biol. *16*, 523–530.

Mazzone, M., Dettori, D., Leite de Oliveira, R., Loges, S., Schmidt, T., Jonckx, B., Tian, Y.M., Lanahan, A.A., Pollard, P., Ruiz de Almodovar, C., et al. (2009). Heterozygous deficiency of PHD2 restores tumor oxygenation and inhibits metastasis via endothelial normalization. Cell *136*, 839–851.

Mortimer, S.A., and Weeks, K.M. (2009). Time-resolved RNA SHAPE chemistry: quantitative RNA structure analysis in one-second snapshots and at single-nucleotide resolution. Nat. Protoc. *4*, 1413–1421.

Pestova, T.V., Kolupaeva, V.G., Lomakin, I.B., Pilipenko, E.V., Shatsky, I.N., Agol, V.I., and Hellen, C.U. (2001). Molecular mechanisms of translation initiation in eukaryotes. Proc. Natl. Acad. Sci. USA *98*, 7029–7036.

Pilipenko, E.V., Pestova, T.V., Kolupaeva, V.G., Khitrina, E.V., Poperechnaya, A.N., Agol, V.I., and Hellen, C.U. (2000). A cell cycle-dependent protein serves as a template-specific translation initiation factor. Genes Dev. *14*, 2028–2045.

Pulaski, B.A., and Ostrand-Rosenberg, S. (2001). Mouse 4T1 breast tumor model. Curr. Protoc. Immunol. *Chapter 20*, Unit 20.2.

Richter, J.D., and Sonenberg, N. (2005). Regulation of cap-dependent translation by eIF4E inhibitory proteins. Nature *433*, 477–480.

Sachs, A.B. (2000). Cell cycle-dependent translation initiation: IRES elements prevail. Cell *101*, 243–245.

Sanz, M.A., Redondo, N., García-Moreno, M., and Carrasco, L. (2013). Phosphorylation of eIF2α is responsible for the failure of the picornavirus internal ribosome entry site to direct translation from Sindbis virus replicons. J. Gen. Virol. *94*, 796–806.Phosphorylation of eIF2α is responsible for the failure of the picornavirus internal ribosome entry site to direct translation from Sindbis virus replicons.

Schito, L., Rey, S., Tafani, M., Zhang, H., Wong, C.C., Russo, A., Russo, M.A., and Semenza, G.L. (2012). Hypoxia-inducible factor 1-dependent expression

of platelet-derived growth factor B promotes lymphatic metastasis of hypoxic breast cancer cells. Proc. Natl. Acad. Sci. USA *109*, E2707–E2716.

Schoppmann, S.F., Fenzl, A., Schindl, M., Bachleitner-Hofmann, T., Nagy, K., Gnant, M., Horvat, R., Jakesz, R., and Birner, P. (2006). Hypoxia inducible factor-1alpha correlates with VEGF-C expression and lymphangiogenesis in breast cancer. Breast Cancer Res. Treat. *99*, 135–141.

Semenza, G.L. (2012). Hypoxia-inducible factors in physiology and medicine. Cell *148*, 399–408.

Silvera, D., and Schneider, R.J. (2009). Inflammatory breast cancer cells are constitutively adapted to hypoxia. Cell Cycle *8*, 3091–3096.

Spriggs, K.A., Stoneley, M., Bushell, M., and Willis, A.E. (2008). Re-programming of translation following cell stress allows IRES-mediated translation to predominate. Biol. Cell *100*, 27–38.

Spriggs, K.A., Bushell, M., and Willis, A.E. (2010). Translational regulation of gene expression during conditions of cell stress. Mol. Cell *40*, 228–237.

Tao, J., Li, T., Li, K., Xiong, J., Yang, Z., Wu, H., and Wang, C. (2006). Effect of HIF-1alpha on VEGF-C induced lymphangiogenesis and lymph nodes metastases of pancreatic cancer. J. Huazhong Univ. Sci. Technolog. Med. Sci. *26*, 562–564.

Vagner, S., Galy, B., and Pyronnet, S. (2001). Irresistible IRES. Attracting the translation machinery to internal ribosome entry sites. EMBO Rep. *2*, 893–898.

Yi, T., Papadopoulos, E., Hagner, P.R., and Wagner, G. (2013). Hypoxia-inducible factor-1α (HIF-1α) promotes cap-dependent translation of selective mRNAs through up-regulating initiation factor eIF4E1 in breast cancer cells under hypoxia conditions. J. Biol. Chem. *288*, 18732–18742.

Zhou, B., Si, W., Su, Z., Deng, W., Tu, X., and Wang, Q. (2013). Transcriptional activation of the Prox1 gene by HIF-1α and HIF-2α in response to hypoxia. FEBS Lett. *587*, 724–731.